Heredity

Heredity (2012) 109, 63–70

www.nature.com/hdy

ORIGINAL ARTICLE

CD36-deficient congenic strains show improved glucose tolerance and distinct shifts in metabolic and transcriptomic profiles

L Šedová[1], F Liška[1], D Křenová[1], L Kazdová[2], J Tremblay[3], M Krupková[1], G Corbeil[3], P Hamet[3], V Křen[1] and O Šeda[1,3]

Deficiency of fatty acid translocase Cd36 has been shown to have a major role in the pathogenesis of metabolic syndrome in the spontaneously hypertensive rat (SHR). We have tested the hypothesis that the effects of *Cd36* mutation on the features of metabolic syndrome are contextually dependent on genomic background. We have derived two new congenic strains by introgression of limited chromosome 4 regions of SHR origin, both including the defective *Cd36* gene, into the genetic background of a highly inbred model of insulin resistance and dyslipidemia, polydactylous (PD) rat strain. We subjected standard diet-fed adult males of PD and the congenic PD.SHR4 strains to metabolic, morphometric and transcriptomic profiling. We observed significantly improved glucose tolerance and lower fasting insulin levels in PD.SHR4 congenics than in PD. One of the PD.SHR4 strains showed lower triglyceride concentrations across major lipoprotein fractions combined with higher levels of low-density lipoprotein cholesterol compared with the PD progenitor. The hepatic transcriptome assessment revealed a network of genes differentially expressed between PD and PD.SHR4 with significant enrichment by members of the circadian rhythmicity pathway (Arntl (Bmal1), Clock, Nfil3, Per2 and Per3). In summary, the introduction of the chromosome 4 region of SHR origin including defective *Cd36* into the PD genetic background resulted in disconnected shifts of metabolic profile along with distinct changes in hepatic transcriptome. The synthesis of the current results with those obtained in other *Cd36*-deficient strains indicates that the eventual metabolic effect of a deleterious mutation such as that of SHR-derived Cd36 is not absolute, but rather a function of complex interactions between environmental and genomic background, upon which it operates.
Heredity (2012) **109,** 63–70; doi:10.1038/hdy.2012.14; published online 4 April 2012

Keywords: functional genomics; metabolic syndrome; animal model; transcriptomics

INTRODUCTION

Metabolic syndrome is a complex human condition with rising prevalence worldwide. Recently, several previously used definitions have been merged into a unified definition of the metabolic syndrome (Alberti *et al.*, 2009). This definition lists dyslipidemia, obesity, hypertension and fasting glucose levels among the syndrome's major components. In spite of clear evidence of the ecogenomic (genome × environment interactive) nature of the pathogenesis of the syndrome and its individual aspects, the identification of causal genetic variants remains elusive even in the era of large, genome-wide association studies (Kraja *et al.*, 2011). To date, one of the few successfully and positionally cloned culprits linked to many facets of the metabolic syndrome is a gene coding for fatty acid translocase *Cd36*, mutation of which has been originally found in the spontaneously hypertensive rat (SHR) (Aitman *et al.*, 1997, 1999; Pravenec *et al.*, 2001). Interestingly, the complex nature of mutation of *Cd36* (a chimeric gene owing to unequal recombination between the *Cd36* gene and one of its pseudogenes) in SHR (Glazier *et al.*, 2002) does not result in complete lack of expression, but rather in severe, tissue-specific downregulation of the gene (Bonen *et al.*, 2009). Although rare, complete deficiencies of Cd36 were reported in humans (Yamamoto *et al.*, 1994; Kashiwagi *et al.*, 1996) and a murine model featuring complete knockout of *Cd36* is available (Febbraio *et al.*, 1999), models carrying the 'incomplete' type of mutation may relevantly represent the more subtle functional consequences of common polymorphisms in human *Cd36* gene. Actually, several single-nucleotide polymorphisms in the human *Cd36* gene were recently associated with lipid levels, metabolic syndrome (Love-Gregory *et al.*, 2008; Noel *et al.*, 2010) or obesity (Bokor *et al.*, 2010), although the latter has not been unanimously confirmed (Choquet *et al.*, 2010).

We have previously shown that introgression of rat chromosome 4 segment including the mutant *Cd36* gene from SHR into the Brown Norway genome results in deterioration of insulin sensitivity and increase in triacylglycerol and free fatty acid levels in the BN.SHR4 congenic strain (Seda *et al.*, 2002). Furthermore, we have found this

[1]Institute of Biology and Medical Genetics, First Faculty of Medicine, Charles University in Prague and General Teaching Hospital, Prague, Czech Republic; [2]Department of Metabolism and Diabetes, Institute for Clinical and Experimental Medicine, Prague, Czech Republic and [3]Centre de recherche, Centre hospitalier de l'Université de Montréal (CRCHUM)—Technôpole Angus, Montreal, Quebec, Canada
Correspondence: Dr O Šeda, Institute of Biology and Medical Genetics, First Faculty of Medicine, Charles University in Prague, Albertov 4, 12800, Prague 2, Czech Republic. E-mail: oseda@lf1.cuni.cz
Received 4 January 2012; revised 22 February 2012; accepted 28 February 2012; published online 4 April 2012

limited portion of genome to be crucial for several pharmacogenetic interactions involving the insulin sensitizer rosiglitazone (Seda *et al.*, 2003a, 2008) and glucocorticoid dexamethasone (Krupkova *et al.*, 2010). In SHR, *Cd36* was established as a key determinant of the insulin-sensitizing actions of thiazolidinediones using SHR transgenic and congenic strains expressing wild-type *Cd36* (Qi *et al.*, 2002). In this study, we have tested the metabolic and transcriptomic impact of the presence of defective *Cd36* within the genomic background of a highly inbred model of metabolic syndrome, the polydactylous rat (Kren, 1975; Sedova *et al.*, 2000). The choice was driven by our previous differential linkage study conducted in PD × BN.SHR4 cross, in which we mapped several suggestive and significant quantitative-trait loci of metabolic syndrome-related traits in the region of *Cd36/Fat* gene (Seda *et al.*, 2003b).

MATERIALS AND METHODS

Rat strains

The polydactylous rat strain (PD/Cub, PD hereafter, Rat Genome Database (Dwinell *et al.*, 2009) (RGD) ID no. 728161) is a highly inbred strain ($F>90$) showing metabolic syndrome attributes (Sedova *et al.*, 2000; Seda *et al.*, 2005), kept since 1969 at the Institute of Biology and Medical Genetics, First Faculty of Medicine, Charles University in Prague (Kren, 1975). In this study, we have established two new congenic strains combining the genomic information of two established genetic models of metabolic syndrome, PD and the spontaneously hypertensive rat (SHR/OlaIpcv, SHR hereafter, RGD ID no. 631848). Such a combination was achieved by introgression of the chromosome 4 segment of SHR origin into the PD genetic background, using marker-assisted backcross breeding. After verifying the congenicity of both the new strains by a whole-genomic marker scan, we precisely defined the extent of SHR-derived regions by genotyping 54 polymorphic microsatellite markers (Table 1).

Experimental protocol

Our study was performed in conformity with the Animal Protection Law of the Czech Republic (311/1997), which is in compliance with the European Community Council recommendations for the use of laboratory animals 86/609/ECC and was approved by the Ethical committee of the First Faculty of Medicine. Adult rat males were held under temperature- and humidity-controlled conditions on a 12-h/12-h light–dark cycle. Throughout the study, the animals had free access to food (standard chow) and water. At the age of 4 months, adult males of both congenic strains and the parental strain PD ($n=6$–8 per strain) were subjected to oral glucose-tolerance test after overnight fasting and the blood samples for other metabolic measurements were drawn. Then the animals were killed and the total weight and the weight of heart, liver, kidneys, adrenals, epididymal and retroperitoneal fat pads were determined; liver tissue was snap frozen in liquid nitrogen for further analyses of gene expression.

DNA extraction, genotyping

PCR was used for genotyping markers polymorphic between progenitor strains. We tested the DNA of both congenic strains (PD.SHR4a, $n=8$; PD.SHR4b, $n=6$) and the progenitor strains PD/Cub and SHR. The rat DNA was isolated by a modified phenol-extraction method from tail-incision samples. Nucleotide sequences of primers were obtained from public databases (RGD, http://rgd.mcw.edu/, The Welcome Trust Centre for Human Genetics, http://www.well.ox.ac.uk/ or Whitehead Institute/MIT Center for Genome Research, http://www-genome.wi.mit.edu/). The PCR products were separated on polyacrylamide (7–10%) gels, detected in ultraviolet light after ethidium-bromide staining using Syngene G:Box.

Metabolic measurements

The oral glucose-tolerance test (OGTT) was performed after overnight fasting and the blood samples for the glycemia determination (Ascensia Elite Blood Glucose Meter; Bayer HealthCare, Mishawaka, IN, USA, validated by Institute of Clinical Biochemistry and Laboratory Diagnostics of the First Faculty of Medicine) were obtained from the tail vein at intervals of 0, 30, 60, 120 and 180 min after intragastric glucose administration to conscious rats ($3\,g\,kg^{-1}$ body weight, 30% aqueous solution). The lipid profile (cholesterol and triglyceride blood concentration in 20 lipoprotein fractions, glycerol level and chylomicron, very-low-density lipoprotein (VLDL), low-density lipoprotein (LDL) and high-density lipoprotein particle sizes) was assessed by high-performance liquid chromatography (HPLC) as described previously (Krupkova *et al.*, 2010; Usui *et al.*, 2002). Serum free fatty acids were determined using an acyl-CoA oxidase-based colorimetric kit (Roche Diagnostics GmbH, Mannheim, Germany). Serum insulin concentration was determined using an ELISA kit for rat insulin assay (Mercodia, Uppsala, Sweden). Serum levels of adiponectin were determined using Rat Adiponectin ELISA kit (B-Bridge International, Cupertino, CA, USA).

Transcriptomic profiling and quantitative real-time PCR

Total RNA was extracted with TRIzol reagent (Invitrogen, Carlsbad, CA, USA) and purified with the RNeasy MinElute cleanup kit (Qiagen, Valencia, CA, USA) following the manufacturer's recommendations. The quality of the total RNA was evaluated on an Agilent 2100 Bioanalyzer system (Agilent, Palo Alto, CA, USA). Microarray experiments were performed using the GeneChip Rat Exon 1.0 ST array (interrogates over 850 000 exon clusters), with approximately four probes per exon and roughly 40 probes per gene (Affymetrix, Santa Clara, CA, USA). Following the ribosomal reduction procedure (Invitrogen), from 1 μg total RNA, each sample was processed using the GeneChip Whole Transcript Sense Target Labeling Assay (Affymetrix). Briefly, after the rRNA reduction procedure, double-stranded cDNA was synthesized with random hexamers tagged with a T7 promoter sequence, then it was amplified by T7 RNA polymerase producing complementary RNA; in the second cycle of cDNA synthesis, complementary RNA was used to produce sense single-stranded cDNA and 5.5 μg was fragmented, labeled and hybridized onto the chip (PD.SHR4a–2 chips; PD–3 chips). The whole hybridization procedure was performed using the Affymetrix GeneChip system according to the protocol recommended by Affymetrix. The hybridization was evaluated with Affymetrix GeneChip Command Console Software (AGCC) and the quality of the chips with Affymetrix Expression Console. Partek Genomics Suite (Partek, St Louis, MO, USA) was used for data analysis. The data were normalized by using Robust Multichip Average (RMA) algorithm, which uses background adjustment, quantile normalization and summarization.

To validate microarray gene expression data, quantitative real-time PCR (SYBR-Green) was used. Total RNA (2 μg) was reverse-transcribed with random primers using the SuperScript VILO cDNA Synthesis Kit (Invitrogen). Primers were designed using Primer3 (Rozen and Skaletsky, 2000) and synthesized by Integrated DNA Technologies. The primer sequences are listed in Supplementary Table 2. Real-time PCR reaction was performed in quadruplicate with EXPRESS SYBR GreenER qPCR SuperMix with Premixed ROX Kit according to the manufacturer's protocol (Invitrogen, Burlington, ON, Canada) using Applied Biosystems (Burlington, ON, Canada) Real-Time PCR System. Results were analyzed using the Pfaffl analysis method (Pfaffl, 2001) with reference genes peptidylprolyl isomerase B and 18S.

Statistical and pathway analyses

The metabolic and morphometric data were compared by one-way analysis of variance with strain as main factor followed by Tukey's honest significance difference test for detailed pair-wise comparison.

Transcriptomic data

After evaluation of the hybridization, the quality control and the data normalization by robust multi-array analysis (RMA), the gene expression was compared between the PD.SHR4a and PD strains using Partek Genomics Suite (Partek). The transcripts found to be significantly differentially expressed between PD and PD.SHR4a strains (FDR <0.1, $n=172$) were included in the gene enrichment and pathway/network analyses, which were performed using web-based DAVID functional enrichment analysis (Huang da *et al.*, 2009) and Ingenuity Pathway Analysis software v.9 applications.

RESULTS

Genomic characteristics of the differential segments in the new PD.SHR4 congenic strains

Our genotyping scan of 54 polymorphic microsatellite markers revealed the extent of the chromosome 4 differential segments of SHR origin in the two PD.SHR4 congenic strains (Table 1). In PD.SHR(D4Arb13-D4Rat125)—PD.SHR4a hereafter—the SHR-derived segment spans about 21 Mb, while in PD.SHR(cen-*Lmbr*; D4Rat147–D4Rat151)—PD.SHR4b hereafter—the introgressed segment is discontinuous as it extends 37 Mb from the centromere with a limited interruption at 1.3–2.4 Mb (Table 1). Several total genome scans conducted throughout the PD.SHR4 strains derivation eventually excluded the presence of other non-PD alleles than those fixed on chromosome 4, confirming the congenicity of the new strains. The SHR-derived segments on chromosome 4 hence represent the only genomic differences between PD and PD.SHR4 congenic strains.

Table 1 Definition of the differential segments in the new PD.SHR4 congenic strains

Marker	*Mbp*	*PD.SHR4a*	*PD.SHR4b*	*Selected genes differing in origin between PD.SHR4a and PD.SHR4b*
D4Rat248	0.28	PD	SHR	
D4Arb14	0.45	PD	SHR	
Il6	0.46	PD	SHR	*Il6*
D4Rat117	1.18	PD	SHR	*Dnajb6*
Lmbr1_i4	1.25	PD	SHR	*Ube3c*
Lmbr_i5_120-816	1.26	PD	SHR	*Lmbr*
D4Mgh7	1.55	PD	PD	
D4Rat147	2.45	PD	SHR	*Shh, En2, Insig1*
D4Rat139	3.04	PD	SHR	*Htr5a, Paxip1, Dpp6*
D4Arb13	3.17	SHR	SHR	
D4Rat4	3.23	SHR	SHR	
D4Rat142	4.82	SHR	SHR	
D4Rat2	5.43	SHR	SHR	
D4Bro1	6.12	SHR	SHR	
D4Rat1	6.69	SHR	SHR	
D4Rat136	8.48	SHR	SHR	
D4Rat5	9.63	SHR	SHR	
D4Rat148	9.68	SHR	SHR	
D4Rat6	10.29	SHR	SHR	
D4Rat7	10.67	SHR	SHR	*Cd36*
D4Rat221	14.38	SHR	SHR	
D4Rat222	19.03	SHR	SHR	
D4Rat125	19.46	SHR	SHR	
D4Rat10	26.29	PD	SHR	*Grm3, Abcb1a, Abcb1b, Crot*
D4Rat151	29.44	PD	SHR	*Cyp51, Pex1, Cdk6, Pon1*
D4Rat17	46.03	PD	PD	
D4Rat16	49.33	PD	PD	
D4Rat119	63.10	PD	PD	
D4Rat102	66.49	PD	PD	
D4Rat27	71.71	PD	PD	
D4Rat28	75.34	PD	PD	
D4Rat168	77.42	PD	PD	
D4Mit24	78.32	PD	PD	
D4Rat33	80.47	PD	PD	
D4Rat34	85.25	PD	PD	
D4Rat35	91.57	PD	PD	
D4Rat172	95.16	PD	PD	
D4Rat39	104.44	PD	PD	
D4Rat175	106.72	PD	PD	
D4Rat97	111.29	PD	PD	
D4Rat176	116.55	PD	PD	
D4Rat53	126.31	PD	PD	
D4Rat80	132.50	PD	PD	
D4Rat58	136.33	PD	PD	
D4Rat196	143.99	PD	PD	
D4Rat60	149.80	PD	PD	
D4Rat59	150.28	PD	PD	
D4Rat137	155.58	PD	PD	
D4Rat203	161.67	PD	PD	
D4Arb27	164.84	PD	PD	
D4Rat68	172.40	PD	PD	
D4Rat69	175.18	PD	PD	
D4Rat140	182.98	PD	PD	
D4Rat72	186.34	PD	PD	

Abbreviations: PD, polydactylous; SHR, spontaneously hypertensive rat.

Morphometry and basic metabolic profile

The PD and the two PD.SHR4 strains did not show any differences in body weight, adipose tissue distribution or relative weights of internal organs except for the slightly lower liver weight in PD.SHR4a (Table 2). Both congenic strains displayed significantly lower levels of fasting plasma glucose and insulin, as well as an overall amelioration of glucose tolerance compared with the PD progenitor (Figure 1). The concentrations of plasma adiponectin and free fatty acids were comparable among the three strains, while free glycerol was significantly lower in both PD.SHR4a and PD.SHR4b congenics (Table 2).

Detailed lipid profile

We observed significantly lower total triglyceride (TG) concentration in PD.SHR4a compared to PD, particularly driven by 43% and 22% differences in VLDL and LDL fractions, respectively (Table 3, Figure 2a). The same, yet less pronounced trend towards lower TG was present in PD.SHR4b, reaching statistical significance only for LDL and high-density lipoprotein fractions (Table 3, Figure 2a). While the total cholesterol was comparable between PD and PD.SHR4a congenic strain, upon a detailed analysis we observed significant elevation of LDL cholesterol in the congenic, unique to this strain (Table 3, Figure 2b). Total cholesterol was lower in PD.SHR4b compared to PD, mostly due to lower concentrations of high-density lipoprotein cholesterol (Table 3, Figure 2b). Only PD.SHR4b showed somewhat altered sizes of lipoprotein particles with larger VLDL compared to both PD and PD.SHR4a and smaller LDL particles compared to PD.SHR4a only (Supplementary Table 1).

Liver transcriptome comparison

As the PD.SHR4a strain carries a substantially smaller chromosome 4 differential segment compared to PD.SHR4b (Table 1) and at the same time it displayed more profound shifts in its metabolic profile, we decided to contrast its hepatic transcriptome with that of the PD rat. After filtering the results for quality parameters and adjusting

Table 2 Morphometric profile of PD versus PD.SHR4 congenic rats

Trait	*PD*	*PD.SHR4a*	*PD.SHR4b*	P_{ANOVA}
N	8	8	6	
Body weight, g	317 ± 6	313 ± 11	297 ± 9	*0.18*
Liver wt., g per 100 g b.wt.	3.11 ± 0.04	2.93 ± 0.02	3.13 ± 0.02[a]	**0.004**
Heart wt., g per 100 g b.wt.	0.29 ± 0.002	0.29 ± 0.01	0.28 ± 0.01	*0.96*
Kidney wt., g per 100 g b.wt.	0.62 ± 0.01	0.61 ± 0.01	0.63 ± 0.01	*0.35*
Adrenals wt., mg per 100 g b.wt.	17.9 ± 0.8	16.7 ± 0.2	17.3 ± 0.5	*0.17*
EFP wt., g per 100 g b.wt.	1.45 ± 0.12	1.36 ± 0.12	1.36 ± 0.07	*0.79*
RFP wt., g per 100 g b.wt.	1.37 ± 0.17	1.29 ± 0.13	1.08 ± 0.16	*0.54*
FFA, mmol l^{-1}	0.75 ± 0.01	0.80 ± 0.04	0.72 ± 0.05	*0.29*
Fasting adiponectin, μg ml^{-1}	3.2 ± 0.6	3.5 ± 0.6	4.0 ± 1.0	*0.77*
Free glycerol, mg dl^{-1}	7.4 ± 0.3	5.1 ± 0.2‡	5.2 ± 0.4†	**0.0004**

Abbreviations: b.wt., body weight; EFP, epidymal fat pad; FFA, free faty acids; PD, polydactylous; RFP, retroperitoneal fat pad; SHR, spontaneously hypertensive rat.
Morphometric profile of PD versus PD.SHR4a and PD.SHR4b male rats fed standard diet. Values are shown as mean ± s.e.m. The significance levels of pair-wise, inter-strain comparisons between PD.SHR4 congenic strains versus PD are shown for post-hoc Tukey's HSD test as follows: †$P<0.01$; ‡$P<0.001$ and [a]$P<0.05$ for the differences between PD.SHR4a and PD.SHR4b. Bold values indicate significant ANOVA result, italic values indicate non-significant ANOVA results.

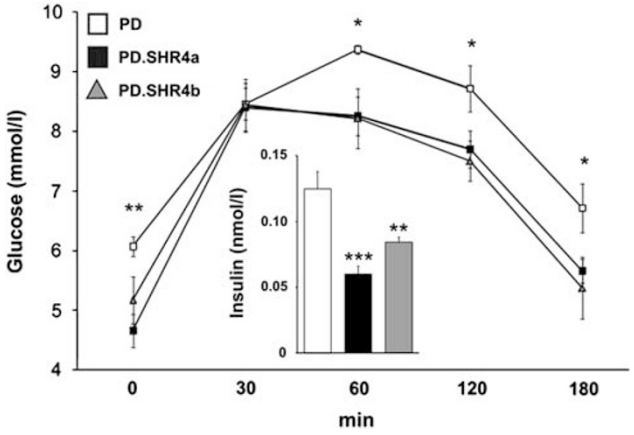

Figure 1 The glucose tolerance and fasting insulin in PD vs PD.SHR4 congenic strains. The course of glycemic curves in PD (white squares) vs PD.SHR4a (black squares) and PD.SHR4b (gray triangles) male rats fed standard diet. Fasting insulin concentrations in PD (white bar) vs PD.SHR4a (black bar) and PD.SHR4b (gray bar). Significance levels for oral glucose-tolerance test are given for the factor strain of one-way ANOVA; for fasting insulin, the strain comparison using the *post-hoc* Tukey's honest significance difference test of the one-way ANOVA with strain as major factor is shown as follows: $^{*}P<0.05$; $^{**}P<0.01$; $^{***}P<0.001$.

Table 3 Triacylglycerol and cholesterol concentrations in major lipoprotein subfractions in PD vs PD.SHR4 congenic rats

Trait (mg dl^{-1})	*PD*	*PD.SHR4a*	*PD.SHR4b*	P_{ANOVA}
N	8	8	6	
Total TG	130.3 ± 5.7	82.2 ± 7.2*	98.6 ± 12.7	**0.017**
Chylomicron TG	0.41 ± 0.04	0.42 ± 0.05	0.46 ± 0.07	*0.83*
VLDL-TG	91.8 ± 6.0	52.5 ± 5.6*	71.7 ± 11.2	**0.022**
LDL-TG	30.4 ± 1.4	23.6 ± 1.6*	20.2 ± 1.0†	**0.001**
HDL-TG	7.7 ± 0.3	5.7 ± 0.2†	6.2 ± 0.5*	**0.008**
Cholesterol (C)				
Total C	60.0 ± 1.5	59.0 ± 1.8	51.4 ± 1.6*,^{a}	**0.009**
Chylomicron C	0.03 ± 0.003	0.03 ± 0.01	0.06 ± 0.01^{a}	**0.019**
VLDL-C	5.7 ± 0.4	4.3 ± 0.2	4.1 ± 0.6	*0.07*
LDL-C	13.1 ± 0.7	16.6 ± 0.7*,^{b}	12.0 ± 0.6	**0.0006**
HDL-C	41.1 ± 0.8	38.2 ± 1.5	35.3 ± 1.1*	**0.035**

Abbreviations: PD, polydactylous; SHR, spontaneously hypertensive rat.
Data are shown as mean ± s.e.m. The significance levels of pair-wise, inter-strain comparisons between PD.SHR4 congenic strains and PD are shown for *post-hoc* Tukey's HSD test as follows: $^{*}P<0.05$, $^{\dagger}P<0.01$, $^{a}P<0.05$ and $^{b}P<0.001$, for the differences between PD.SHR4a and PD.SHR4b. Bold values indicate significant ANOVA result, italic values indicate non-significant ANOVA results.

statistical significance levels for multiple comparisons (see Materials and methods), we found 172 transcripts to be differentially expressed between PD and PD.SHR4a (Supplementary Data Set), with 48 of the transcripts showing more than a twofold difference (Table 4a,b). The numbers of transcripts up- and downregulated in PD.SHR4a vs PD were roughly balanced (83 up- vs 89 downregulated). Apart from the expected substantially reduced expression of *Cd36* in the congenic strain, there was no other differentially expressed gene located in the segment of chromosome 4 of SHR origin (Table 4 and Supplemental Data Set). The rest of the differentially expressed genes were spread across almost all the other chromosomes. In order to validate the results of the microarray experiment, we performed quantitative real-time PCR assessment of the expression of nine representative genes: ATP-binding cassette, sub-family G (WHITE), member 5 (*Abcg5*); early growth response 1 (*Egr1*); insulin-like growth factor binding protein 2 (*Igfbp2*); period homolog 2 (Drosophila) (*Per2*); nuclear-receptor subfamily 1, group I, member 3 (*Nr1i3*); apolipoprotein B mRNA editing enzyme, catalytic polypeptide 1 (*Apobec1*); apolipoprotein L, 3 (*Apol3*); insulin induced gene 1 (*Insig1*); and aryl hydrocarbon receptor nuclear translocator-like (*Arntl*). As evident from Supplementary Figure 1, in all cases we were able to confirm the direction of expression change between PD and PD.SHR4a, in most of them the degree of up- or downregulation corresponded well. The relative overexpression of *Igfbp2*, *Per2* and *Nr1i3* in PD.SHR4a was even greater than the one ascertained by microarray.

Pathway/network analysis

Using all 172 significantly differentially expressed genes, we carried out a systematic search for their enrichment in ontological categories, canonical pathways or disease-related gene sets as well as their potential functional connections. First, we examined the degree of over-representation of our set of genes in the canonical pathways using the relevant module in the Ingenuity Pathway Analysis v.9 software. After correction for multiple testing using Benjamini–Hochberg false discovery rate, we identified four pathways significantly enriched by the genes most distinctly expressed in PD vs

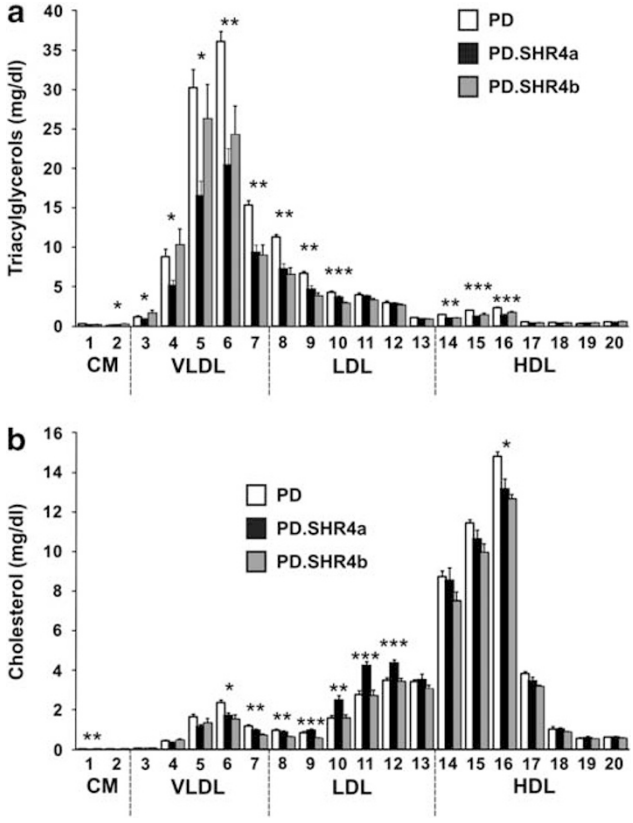

Figure 2 (**a**) The triacylglycerols (**a**) and (**b**) cholesterol content in 20 lipoprotein subfractions in PD (white bars) versus PD.SHR4a (black bars) and PD.SHR4b (gray bars) male rats. Within the graph, the significance levels for strain differences are shown for one-way ANOVA (STRAIN factor) as follows: $^{*}P<0.05$; $^{**}P<0.01$; $^{***}P<0.001$. The allocation of individual lipoprotein subfractions to major lipoprotein classes is shown in order of the particle's decreasing size from left to right. CM, chylomicron; HDL, high-density lipoprotein; LDL, low-density lipoprotein; VLDL, very low-density lipoprotein.

Table 4 List of significantly differentially expressed transcripts between PD and PD.SHR4a (FDR < 0.1, fold change > 2). (a) Genes significantly overexpressed in PD.SHR4 vs PD (fold change > 2); (b) genes significantly underexpressed in PD.SHR4 vs PD (fold change > 2)

Gene symbol	*Gene name*	*Chr.*	*P-value*	*Fold change (PD vs PD.SHR4)*
(a)				
Egr1	Early growth response 1	18q	1.28E −03	17.7
Nat8	*N*-acetyltransferase 8 (GCN5-related, putative)	4q34	1.82E −03	11.5
Abcg5	ATP-binding cassette, sub-family G (WHITE), member 5	6q12	1.82E −04	11.2
Igfbp2	Insulin-like growth factor binding protein 2	9q33	1.04E −04	6.5
Per3	Period homolog 3 (Drosophila)	5q36	1.01E −03	6.5
Nr1i3	nuclear receptor subfamily 1, group I, member 3	13q24	1.47E −03	5.7
Por	P450 (cytochrome) oxidoreductase	12q12	5.62E −04	4.8
Per2	Period homolog 2 (Drosophila)	9q36	1.74E −03	4.6
Aldh1a1	Aldehyde dehydrogenase family 1, member A1	1q51	3.16E −03	4.6
Gcnt2	Glucosaminyl (N-acetyl) transferase 2, I-branching enzyme	17p12	3.49E −04	4.0
Cyp2j2	Cytochrome P450, family 2, subfamily J, polypeptide 2	5q33	8.50E −04	3.6
Pdgfc	Platelet-derived growth factor, C polypeptide	2q33	3.78E −03	2.8
Abcb1a	ATP-binding cassette, sub-family B (MDR/TAP), member 1	4q12	1.08E −03	2.6
Ces2b/Ces2c	carboxylesterase 2C	1q55	7.83E −04	2.6
Tmem8	Rattus norvegicus transmembrane protein 48	10q12	1.85E −04	2.5
Itpr1	Inositol 1,4,5-triphosphate receptor, type 1	4q41	1.62E −03	2.4
Abo	**ABO** blood group (transferase A, alpha 1-3-N-acetylgalactosaminyltransferase; transferase B, alpha 1-3-galactosyltransferase)	3p13	2.12E −03	2.4
Abcd2	ATP-binding cassette, sub-family D (ALD), member 2	7q35	9.16E −05	2.3
C9orf95	Chromosome 9 open reading frame 95	9	6.76E −04	2.3
Herpud1	Homocysteine-inducible, endoplasmic reticulum stress-inducible, ubiquitin-like domain member 1	19p12	1.39E −03	2.1
Pnpla7	Patatin-like phospholipase domain containing 7	3p13	2.00E −03	2.1
(b)				
Arntl	Aryl hydrocarbon receptor nuclear translocator-like	1q34	1.72E −03	−13.5
Cd36	Cd36/Fatty acid translocase	4q11	3.08E −04	−11.7
Insig1	insulin induced gene 1	4q11	1.87E −03	−10.0
Phf11	PHD finger protein 11	15p12	1.76E −03	−9.6
Acpp	Acid phosphatase, prostate	8q32	5.32E −04	−7.0
Apol3	Apolipoprotein L, 3	7q34	2.37E −04	−6.9
Srd5a1	Steroid-5-alpha-reductase, alpha polypeptide 1 (3-oxo-5 alpha-steroid delta 4-dehydrogenase alpha 1)	17p14	9.26E −04	−6.7
Slc34a2	Solute carrier family 34 (sodium phosphate), member 2	14q11	7.86E −04	−6.1
Ltc4s	Leukotriene C4 synthase	10q22	1.05E −03	−5.7
LOC360228	WDNM1 homolog	10q26	5.29E −04	−5.3
Nfil3	Nuclear factor, interleukin 3 regulated	17p14	3.00E −03	−4.7
Psmb8	Proteasome (prosome, macropain) subunit, beta type 8 (large multifunctional peptidase 7)	20p12	1.89E −03	−3.1
RGD1304580	Similar to Hypothetical protein MGC38513	1q21	1.35E −03	−2.9
Cxadr	Coxsackie virus and adenovirus receptor	11q11	4.83E −04	−2.7
Capg	capping protein (actin filament), gelsolin-like	4q33	3.78E −03	−2.7
Oprs1	Opioid receptor, sigma 1	5q22	1.98E −03	−2.6
Hamp	Hepcidin antimicrobial peptide	1q21	2.43E −03	−2.5
Casp1	Caspase 1	8q11	3.25E −03	−2.5
C6	Complement component 6	2q16	1.01E −03	−2.5
Trim5	Tripartite motif-containing 5	1q32	9.38E −04	−2.3
Tspo	Translocator protein	7q34	3.56E −04	−2.3
Apobec1	Apolipoprotein B mRNA editing enzyme, catalytic polypeptide 1	4q42	3.07E −03	−2.3
Bst2	Bone marrow stromal cell antigen 2	16p14	8.53E −04	−2.2
Pgrmc2	Progesterone receptor membrane component 2	2q26	3.58E −03	−2.2
Vwa5a	Von Willebrand factor A domain containing 5A	8q22	3.16E −03	−2.1
Gtf2ird1	GTF2I repeat domain containing 1	12q12	4.54E −05	−2.0
Anxa3	Annexin A3	14p22	1.32E −05	−2.0

The *P*-value is adjusted for multiple comparisons.

PD.SHR4: circadian rhythm signaling, xenobiotic metabolism signaling, PXR/RXR activation and LPS/IL-1-mediated inhibition of RXR function (Supplementary Figure 2). In the subsequent toxicity functions analysis (as implemented in IPA), only liver regeneration, liver steatosis and renal tubule injury surpassed the statistical threshold for significant over-representation both in the total sample of 172

genes and in the subset upregulated in PD.SHR4. Then, we proceeded to assess the potential functional relations among the genes differentially expressed between PD.SHR4a and PD using dynamic pathway modeling. Both approaches focusing on direct interactions of identified genes or the 'shortest path' among them revealed several major modules, the most prominent being formed by the four major genes involved in circadian rhythmicity (Figure 3).

DISCUSSION

The transfer of a limited segment of rat chromosome 4 including the mutated *Cd36* gene of SHR origin into the genomic background of PD rat strain elicited an improvement in glucose tolerance, lowering of insulinaemia and shifts in lipid levels contrasting with those reported previously after a similar transfer to Brown Norway genomic background (Seda *et al.*, 2002, 2003a; Table 5). As we have previously shown the concentrations of insulin, glucose, free fatty acids and cholesterol to be comparable in PD and SHR strains (Sedova *et al.*, 2000), the current results indicate the presence of an interaction between gene(s) within the introgressed segments and genomic background of the congenic strains.

Although many of the studies including ours demonstrated the association of lack of Cd36 with metabolic syndrome features like insulin resistance or dyslipidemia (Aitman *et al.*, 1997, 1999; Febbraio *et al.*, 1999; Pravenec *et al.*, 2001; Seda *et al.*, 2002), there are also reports suggesting that, in certain circumstances, the expression level of Cd36 actually correlates positively with unfavorable metabolic profile. Recently, it has been shown by Love-Gregory *et al.* (2011) that in African-Americans the Cd36 variants that reduce protein expression appear to promote a protective metabolic profile, particularly concerning high-density lipoprotein and VLDL lipid levels

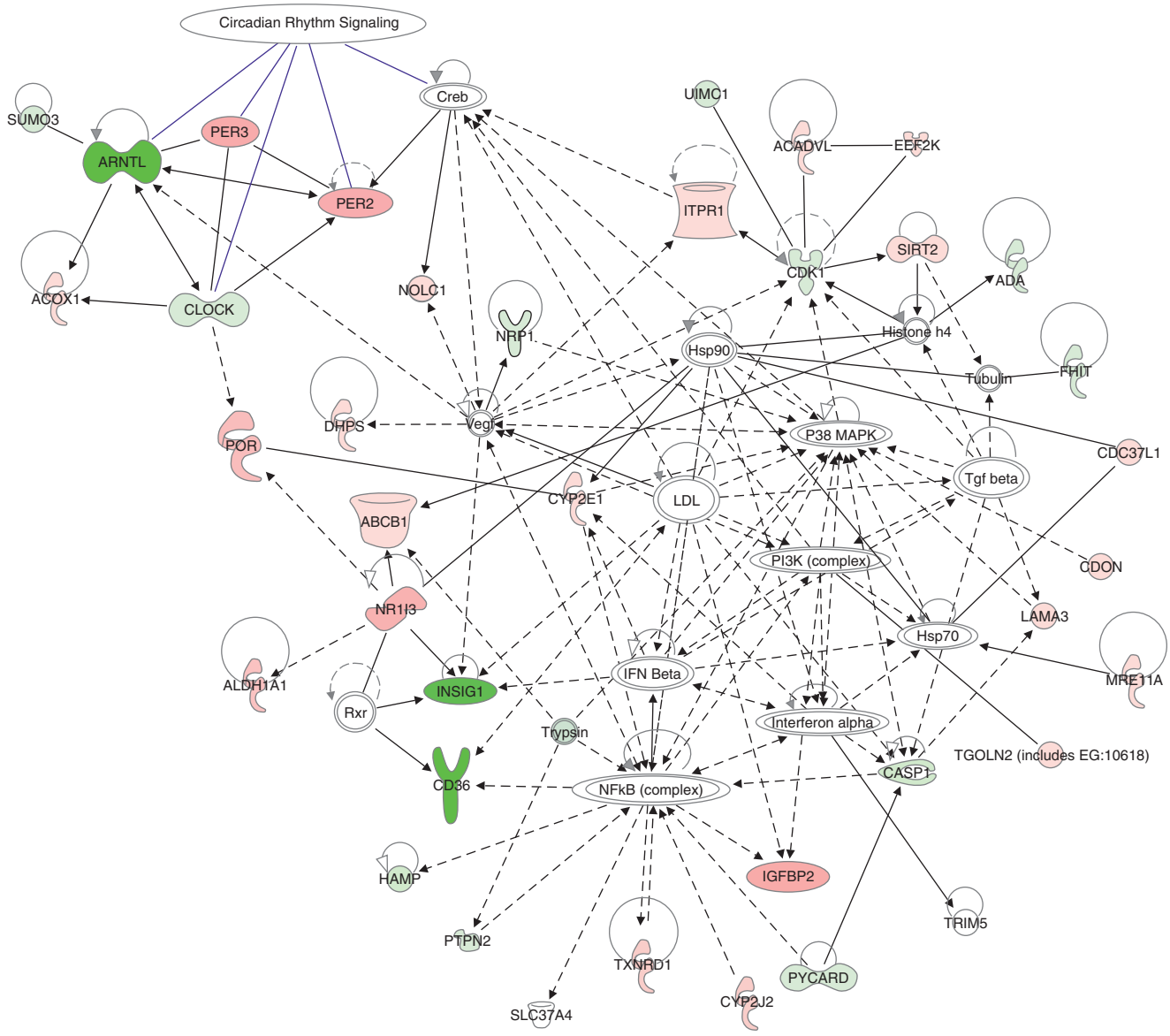

Figure 3 Network analysis of the differentially expressed genes in the livers of PD and PD.SHR4a strains. The figure represents network with the highest score (IPA v.9, Ingenuity Systems) derived using the whole set of differentially expressed genes between PD and PD.SHR4a. The genes relatively downregulated in PD.SHR4a vs PD are shown in shades of green; the genes relatively upregulated in PD.SHR4a vs PD are shown in shades of red (in both cases, the darker the color, the bigger the fold change of expression). The members of the circadian rhythm signaling group are indicated by blue arrows.

(Love-Gregory *et al*., 2011). Also, the *Cd36* knockout mice fed chow diet displayed lower fasting concentrations of glucose and insulin compared with wild-type controls (Hajri *et al*., 2002), similarly to PD.SHR4 congenics in the current study. On the other hand, their triglyceride and free fatty acid levels were increased in contrast to the decrease or no change observed in our study (Table 5). Absence of Cd36 also protects mice from insulin resistance associated with high fat diet-induced obesity and hyperlipidemia (Kennedy *et al*., 2011) and, conversely, increased expression of hepatic Cd36 in response to high fat diet-induced obesity was found to be sufficient to exacerbate hepatic triglyceride storage and secretion (Koonen *et al*., 2007). One of the mechanisms responsible may lie in the fact that human islets express Cd36 in the plasma membrane as well as in the insulin-secretory granules, and Cd36 activity was deemed important for uptake of fatty acids into β-cells as well as for mediating their modulatory effects on insulin secretion (Noushmehr *et al*., 2005) .

Altogether, it is apparent that the eventual metabolic effect of *Cd36* deficiency is tightly linked to a particular setting of both genomic background (for example, PD.SHR4 vs BN.SHR4 (Seda *et al*., 2002, 2003b); Table 5 and Supplementary Figure 3) and environmental factors, particularly diet (Febbraio *et al*., 1999; Hajri *et al*., 2002; Koonen *et al*., 2007; Kennedy *et al*., 2011) or medication (Qi *et al*., 2002; Seda *et al*., 2003a; Seda *et al*., 2008; Krupkova *et al*., 2010). Therefore, the apparently controversial issue of causal relation between level of Cd36 expression and metabolic outcome may be resolved by adoption of broader conceptual framework incorporating other (eco)genomic factors.

Apart from *Cd36*, significant overexpression of *Igfbp2* in PD.SHR4a (yet genetically of PD origin in both strains) represents a possible mediator of the enhanced insulin sensitivity, as was reported, for example, in *Igfbp2* transgenic mice (Wheatcroft *et al*., 2007). The observation of concurrent upregulation of *Abcg5* and down-regulation of *Insig1* in PD.SHR4 congenic follows well their assumed respective roles in cholesterol efflux and its cellular feedback regulation. This shift, reported also in *Insig1* −/−*Insig2* −/− mice (Engelking *et al*., 2005), may suggest a tendency toward increasing lipid deposition in liver, although we did not validate this parameter directly.

One of the intriguing results in the current study was the identification of a differentially expressed set of circadian clock-related genes (Figure 3). The fundamental interrelatedness of circadian rhythmicity, inter- and intra-organ desynchrony with the metabolic and signaling pathways involved in the pathogenesis of cardiometabolic diseases has been supported by an ever-growing body of evidence, reviewed recently in detail elsewhere (Eckel-Mahan and Sassone-Corsi, 2009; Maury *et al*., 2010). The gene most downregulated in PD.SHR4a liver compared with PD was *Arntl* (also known as *Bmal1*), an essential component of master circadian pacemaker (Bunger *et al*., 2000), together with upregulated *Per2* and *Per3* genes, two natural inhibitors of *Bmal1* and parts of its negative-feedback loop. There is a certain resemblance to the studies in liver-specific *Bmal1* knockout mice, which show hypoglycemia restricted to the fasting phase of the daily cycle and enhanced glucose clearance after an overnight fast (Lamia *et al*., 2008), but not reduced fasting-insulin levels, found in both PD.SHR4 congenic strains and complete *Bmal1* knockout (Lamia *et al*., 2008). We are not aware of any previous report functionally linking the metabolic outcomes of *Cd36* polymorphisms to circadian-clock circuitry.

Finally, we observed several differences in lipid levels and liver weight between the two congenic strains. There are several plausible candidates for these effects within the three regions differing between PD.SHR4a and PD.SHRb, namely *Insig1*, serotonin receptor *Htr5a* or carnitine *O*-octanoyltransferase (*Crot*) as indicated in Table 1. We cannot completely exclude the possibility that some of the other genes of SHR origin are present in the differential segment(s) of the congenic PD.SHR4 strains contributed to the observed metabolic effects commonly present in both congenics and SHR. However, the transcriptome analysis and functional annotation of all the genes in the segment reinforce rather the effect of the *Cd36* mutation. Within the differential segment of the PD.SHR4a strain, there are 58 well-documented protein-coding genes (Supplemental Table 3) among about 120 transcripts. Of those, only *Cd36* was found to be differentially expressed between PD and PD.SHR4a. Further studies are needed to assess the effect of Cd36 and the whole differential segment under distinct nutritional and pharmacological challenges, especially given our previous extensive documentation of nutrigenetic and pharmacogenetic interactions of a similar genomic region in the BN.SHR4 congenic strain (Seda *et al*., 2003a, 2008; Krupkova *et al*., 2010). In sum, the introduction of mutated *Cd36* into the genomic background of an inbred model of metabolic syndrome resulted in disconnected shifts of metabolic profile along with distinct changes in hepatic transcriptome. Our network analysis revealed possible pathways underlie the improvement of insulin sensitivity toward a shift in lipid profile. The synthesis of the current results with those obtained in other *Cd36*-deficient strains indicates that the eventual metabolic effect of a deleterious mutation such as that of SHR-derived *Cd36* is not absolute, but rather a function of complex interactions between environment and genomic background, upon which it operates.

Table 5 Comparison of effect of *Cd36* deficiency in different genetic models

	BN.SHR4 vs BN	*PD.SHR4 vs PD*	*Cd36 −/− mice vs WT*
Fasting glucose	↑	↓	↓
Fasting insulin	↑	↓	↓
Fasting TG	↑	↓ ↔	↑
Fasting FFA	↑	↔	↑

Abbreviations: FFA, free fatty acids;TG, triacylglycerols;
Summary of metabolic effects owing to introduction of mutant *Cd36* into different genetic backgrounds. All data are based on reports utilizing standard chow only. The arrows indicate the respective change of the metabolic parameter in the *Cd36*-deficient animals versus their wild-type controls: ↑, increase; ↓, decrease; ↔, no change.

DATA ARCHIVING

Complete microarray datasets have been submitted to the NCBI Gene Expression Omnibus (GEO) under the record GSE33597. Remaining data have been deposited in the Dryad repository: doi:10.5061/dryad.9f8q91q3.

CONFLICT OF INTEREST

The authors declare no conflict of interest.

ACKNOWLEDGEMENTS

We thank Michaela Janků, Barbora Baladová and Marie Uxová for their excellent technical assistance. This work was supported by Research Project MSM 0021620807 and by the scientific programme of Charles University, PRVOUK-P25/LF1/2.

Aitman TJ, Glazier AM, Wallace CA, Cooper LD, Norsworthy PJ, Wahid FN *et al.* (1999). Identification of Cd36 (Fat) as an insulin-resistance gene causing defective fatty acid and glucose metabolism in hypertensive rats. *Nat Genet* **21**: 76–83.

Aitman TJ, Gotoda T, Evans AL, Imrie H, Heath KE, Trembling PM *et al.* (1997). Quantitative trait loci for cellular defects in glucose and fatty acid metabolism in hypertensive rats. *Nat Genet* **16**: 197–201.

Alberti KGMM, Eckel RH, Grundy SM, Zimmet PZ, Cleeman JI, Donato KA *et al.* (2009). Harmonizing the Metabolic Syndrome: A Joint Interim Statement of the International Diabetes Federation Task Force on Epidemiology and Prevention; National Heart, Lung, and Blood Institute; American Heart Association; World Heart Federation; International Atherosclerosis Society; and International Association for the Study of Obesity. *Circulation* 120: 1640–1645.

Bokor S, Legry V, Meirhaeghe A, Ruiz JR, Mauro B, Widhalm K *et al.* (2010) Single-nucleotide polymorphism of CD36 locus and obesity in European adolescents. *Obesity (Silver Spring)* **18**: 1398–1403.

Bonen A, Han XX, Tandon NN, Glatz JF, Lally J, Snook LA *et al.* (2009). FAT/CD36 expression is not ablated in spontaneously hypertensive rats. *J Lipid Res* **50**: 740–748.

Bunger MK, Wilsbacher LD, Moran SM, Clendenin C, Radcliffe LA, Hogenesch JB *et al.* (2000). Mop3 is an essential component of the master circadian pacemaker in mammals. *Cell* **103**: 1009–1017.

Choquet H, Labrune Y, De Graeve F, Hinney A, Hebebrand J, Scherag A *et al.* (2010). Lack of association of CD36 SNPs with early onset obesity: a meta-analysis in 9,973 European subjects. *Obesity (Silver Spring)* **19**: 833–839.

Dwinell MR, Worthey EA, Shimoyama M, Bakir-Gungor B, DePons J, Laulederkind S *et al.* (2009). The Rat Genome Database 2009: variation, ontologies and pathways *Nucleic Acids Res* **37**: D744–749.

Eckel-Mahan K, Sassone-Corsi P (2009). Metabolism control by the circadian clock and vice versa. *Nat Struct Mol Biol* **16**: 462–467.

Engelking LJ, Liang G, Hammer RE, Takaishi K, Kuriyama H, Evers BM *et al.* (2005). Schoenheimer effect explained–feedback regulation of cholesterol synthesis in mice mediated by Insig proteins. *J Clin Invest* **115**: 2489–2498.

Febbraio M, Abumrad NA, Hajjar DP, Sharma K, Cheng W, Pearce SF *et al.* (1999). A null mutation in murine CD36 reveals an important role in fatty acid and lipoprotein metabolism. *J Biol Chem* **274**: 19055–19062.

Glazier AM, Scott J, Aitman TJ (2002). Molecular basis of the Cd36 chromosomal deletion underlying SHR defects in insulin action and fatty acid metabolism. *Mamm Genome* **13**: 108–113.

Hajri T, Han XX, Bonen A, Abumrad NA (2002). Defective fatty acid uptake modulates insulin responsiveness and metabolic responses to diet in CD36-null mice. *J Clin Invest* **109**: 1381–1389.

Huang da W, Sherman BT, Lempicki RA (2009). Systematic and integrative analysis of large gene lists using DAVID bioinformatics resources. *Nat Protoc* **4**: 44–57.

Kashiwagi H, Tomiyama Y, Nozaki S, Honda S, Kosugi S, Shiraga M *et al.* (1996). A Single Nucleotide Insertion in Codon 317 of the CD36 Gene Leads to CD36 Deficiency. *Arterioscler Thromb Vasc Biol* **16**: 1026–1032.

Kennedy DJ, Kuchibhotla S, Westfall KM, Silverstein RL, Morton RE, Febbraio M (2011). A CD36-dependent pathway enhances macrophage and adipose tissue inflammation and impairs insulin signalling. *Cardiovasc Res* **89**: 604–613.

Koonen DPY, Jacobs RL, Febbraio M, Young ME, Soltys C-LM, Ong H *et al.* (2007). Increased hepatic CD36 expression contributes to dyslipidemia associated with diet-induced obesity. *Diabetes* **56**: 2863–2871.

Kraja AT, Vaidya D, Pankow JS, Goodarzi MO, Assimes TL, Kullo IJ *et al.* (2011) A bivariate genome-wide approach to metabolic syndrome: STAMPEED Consortium. *Diabetes* **60**: 1329–1339.

Kren V (1975). Genetics of the polydactyly-luxate syndrome in the Norway rat, Rattus norvegicus. *Acta Univ Carol Med Monogr* 1–103.

Krupkova M, Sedova L, Liska F, Krenova D, Kren V, Seda O (2010). Pharmacogenetic interaction between dexamethasone and Cd36-deficient segment of spontaneously hypertensive rat chromosome 4 affects triacylglycerol and cholesterol distribution into lipoprotein fractions. *Lipids Health Dis* **9**: 38.

Lamia KA, Storch KF, Weitz CJ (2008). Physiological significance of a peripheral tissue circadian clock. *Proc Natl Acad Sci U S A* **105**: 15172–15177.

Love-Gregory L, Sherva R, Schappe T, Qi JS, McCrea J, Klein S *et al.* (2011). Common CD36 SNPs reduce protein expression and may contribute to a protective atherogenic profile. *Hum Mol Genet* **20**: 193–201.

Love-Gregory L, Sherva R, Sun L, Wasson J, Schappe T, Doria A *et al.* (2008). Variants in the CD36 gene associate with the metabolic syndrome and high-density lipoprotein cholesterol. *Hum Mol Genet* **17**: 1695–1704.

Maury E, Ramsey KM, Bass J (2010). Circadian rhythms and metabolic syndrome: from experimental genetics to human disease. *Circ Res* **106**: 447–462.

Noel SE, Lai CQ, Mattei J, Parnell LD, Ordovas JM, Tucker KL (2010). Variants of the CD36 gene and metabolic syndrome in Boston Puerto Rican adults. *Atherosclerosis* **211**: 210–215.

Noushmehr H, D'Amico E, Farilla L, Hui H, Wawrowsky KA, Mlynarski W *et al.* (2005). Fatty acid translocase (FAT/CD36) is localized on insulin-containing granules in human pancreatic beta-cells and mediates fatty acid effects on insulin secretion. *Diabetes* **54**: 472–481.

Pfaffl MW (2001). A new mathematical model for relative quantification in real-time RT-PCR. *Nucleic Acids Res* **29**: e45.

Pravenec M, Landa V, Zidek V, Musilova A, Kren V, Kazdova L *et al.* (2001). Transgenic rescue of defective Cd36 ameliorates insulin resistance in spontaneously hypertensive rats. *Nat Genet* **27**: 156–158.

Qi N, Kazdova L, Zidek V, Landa V, Kren V, Pershadsingh HA *et al.* (2002). Pharmacogenetic evidence that cd36 is a key determinant of the metabolic effects of pioglitazone. *J Biol Chem* **277**: 48501–48507.

Rozen S, Skaletsky H (2000). Primer3 on the WWW for general users and for biologist programmers. *Methods Mol Biol* **132**: 365–386.

Seda O, Kazdova L, Krenova D, Kren V (2003a). Rosiglitazone fails to improve hypertriglyceridemia and glucose tolerance in CD36-deficient BN.SHR4 congenic rat strain. *Physiol Genomics* **12**: 73–78.

Seda O, Liska F, Krenova D, Kazdova L, Sedova L, Zima T *et al.* (2005). Dynamic genetic architecture of metabolic syndrome attributes in the rat. *Physiol Genomics* **21**: 243–252.

Seda O, Liska F, Krenova D, Kazdova L, Sedova L, Zima T *et al.* (2003b). Differential linkage of triglyceride and glucose levels on rat chromosome 4 in two segregating rat populations. *Folia Biol (Praha)* **49**: 223–226.

Seda O, Sedova L, Kazdova L, Krenova D, Kren V (2002). Metabolic characterization of insulin resistance syndrome feature loci in three brown Norway-derived congenic strains. *Folia Biol (Praha)* **48**: 81–88.

Seda O, Sedova L, Oliyarnyk O, Kazdova L, Krenova D, Corbeil G *et al.* (2008). Pharmacogenomics of metabolic effects of rosiglitazone. *Pharmacogenomics* **9**: 141–155.

Sedova L, Kazdova L, Seda O, Krenova D, Kren V (2000). Rat inbred PD/cub strain as a model of dyslipidemia and insulin resistance. *Folia Biol (Praha)* **46**: 99–106.

Usui S, Hara Y, Hosaki S, Okazaki M (2002). A new on-line dual enzymatic method for simultaneous quantification of cholesterol and triglycerides in lipoproteins by HPLC *J Lipid Res* **43**: 805–814.

Wheatcroft SB, Kearney MT, Shah AM, Ezzat VA, Miell JR, Modo M *et al.* (2007). IGF-binding protein-2 protects against the development of obesity and insulin resistance. *Diabetes* **56**: 285–294.

Yamamoto N, Akamatsu N, Sakuraba H, Yamazaki H, Tanoue K (1994). Platelet glycoprotein IV (CD36) deficiency is associated with the absence (type I) or the presence (type II) of glycoprotein IV on monocytes. *Blood* **83**: 392–397.

Supplementary Information accompanies the paper on Heredity website (http://www.nature.com/hdy)